OKÜ Fen Bilimleri Enstitüsü Dergisi
8(1): 353-374, 2025

OKU Journal of TheInstitute of Science and Technology, 8(1): 353-374, 2025

Osmaniye Korkut Ata Üniversitesi Fen Bilimleri Enstitüsü Dergisi

Osmaniye Korkut Ata University Journal of The Institute of Science and Technology

MIG Kaynağı Yapabilen Robot Kolun Tasarımı ve Kinematik Analizi

Dilşad AKGÜMÜŞ GÖK[1*], Mehmet Furkan ÖZKAN[2], Haydar Emre KARAMAN[3], Mohammad Sami KHATTAB[4]

[1,2,3,4] Istanbul Aydin University Graduate Education Institute Mechanical Engineering, 34320, İstanbul, Türkiye

[1]https://orcid.org/0000-0003-3403-3815
[2]https://orcid.org/0009-0002-8440-5138
[3]https://orcid.org/0009-0001-2154-7959
[4]https://orcid.org/0009-0006-2303-0538
*Sorumlu yazar: dilsadakgumus@aydin.edu.tr

Araştırma Makalesi

Makale Tarihçesi:
Geliş tarihi: 03.07.2024
Kabul tarihi: 26.09.2024
Online Yayınlanma: 15.01.2025

Anahtar Kelimeler:
Robot kol
MIG kaynağı
Kinematik analiz

ÖZ

İnsansız imalat, modern endüstride büyük bir yer edinmiştir. İmalatın insansız olduğu her alanda başarısı ve uygulanabilirliği kanıtlanmıştır. Çeşitli araçlar donanımsal yönden zenginleştirilmiş ve imalat için görevlere uygun hale getirilmiştir. Teknolojinin hızlı gelişimi donanımsal olarak zenginleştirilen bu araçlar için daha fazla donanım kullanma şansı sunmaktadır. Bu donanımlarda en yoğun çalışmalar robot kollar üzerine yapılmaktadır. Bu makale imalat sektöründe, başta otomotiv ve savunma sanayi olmak üzere çeşitli uygulamalar için kullanılmak üzere metal inert gaz (MIG) kaynağı yapabilen robot kol tasarımı üzerine hazırlanmıştır. Çok farklı imalat alanlarında, sistemin altına ya da üstüne tasarımları dikkate alınarak monte edilebilecek bir MIG kaynak robot kolu tasarımı yapılmıştır. Tasarımda insansız kullanılan sistemlerin özellikleri dikkate alınmıştır. Kinematik model, genel dönüşüm, matris, tüm eklem ve birleştirmeleri hesaplanarak oluşturulmuştur. SOLIDWORKS programında tasarımı ve malzeme seçimi yapılan robot kolun, SOLIDWORKS ve ANSYS programlarının kullanımı ile belirli yükler altında deformasyon, hareket ve sapma analizleri yapılmıştır. Bir ve iki numaralı eklemler üzerine yapılan analizler sonucu robot kolun maruz kaldığı yüklerde istenilen kaynak görevlerini yapabileceği görülmüştür.

Design and Kinematic Analysis of a Robotic Arm Capable of MIG Welding

Research Article

Article History:
Received: 03.07.2024
Accepted: 26.09.2024
Published online: 15.01.2025

Keywords:
Robotic arm
MIG welding
Kinematic analysis

ABSTRACT

The importance of unmanned production has grown significantly in modern industry. The success and applicability of manufacturing in unmanned areas have been proven. Various tools have been enriched in terms of hardware and adapted for manufacturing tasks. The rapid development of technology offers the chance to use more hardware for these hardware-enriched tools. The most intense studies in these hardware are conducted on robotic arms. This article has been prepared on the design of a robotic arm capable of metal inert gas (MIG) welding for various applications in the manufacturing sector, especially in the automotive and defense industries. A MIG welding robotic arm design that can be mounted under or over the system in very different manufacturing areas, considering the designs, has been made. The characteristics of unmanned systems used in the design have been taken into account. The kinematic model was created by calculating the general transformation, matrix, all joints, and assemblies. The robotic arm, designed in SOLIDWORKS and material selection made, was analyzed for deformation, motion, and deviation under certain loads using SOLIDWORKS and ANSYS programs. The analyses conducted on the first and second joints showed that

the robotic arm can perform the desired welding tasks under the loads it is subjected to.

To Cite: Gök DA., Özkan MF., Karaman HE., Khattab MS. Design and Kinematic Analysis of a Robotic Arm Capable of MIG Welding. Osmaniye Korkut Ata Üniversitesi Fen Bilimleri Enstitüsü Dergisi 2025; 8(1): 353-374.

1. Introduction

With the advancement of technology, robotic arms with very different hardware can now be used in many challenging tasks (Efe et al., 2021). Due to design simplicity and cost-effectiveness, their production and usage have become easier. Especially, in many areas where human health is at risk, the use of robotic arms is becoming increasingly widespread day by day. The increase in software and system developments for use in different challenging tasks enables robotic arms to be used in very complex jobs. They are used in various areas such as transportation (relocation) (Murat and Abdullah, 2023), firefighting and welding (Doruk et al., 2016), assembly (Karacan et al., 2022), and sorting (separation) (Demirhan and Sarıyıldız, 2021).

Robotic arms are used in many areas, especially in industry. They are preferred, because they reduce the workload and represent the difficult part in human-machine task sharing. Although there are multiple types, the basic tasks performed by robotic arms are very similar to each other. Each robotic arm carries its own unique features. Articulated robotic arms (Bernett et al., 2020), one of the most important types, are robotic arms with a high degree of freedom. These types of high-degree-of-freedom robotic arms are particularly widely used in the automotive industry.

Metal inert gas (MIG) welding is used in many sectors today. Compared to other welding methods, its main advantages include the ability to weld products quickly (Nurveren and Gündüz, 2018), the creation of high-strength products when the craftsmanship is done correctly (Köse and Tatlı, 2015), and most importantly, the ability to fill deep gaps quickly and effectively (Türker et al., 2017). With the benefits brought by its many advantages, high-strength products are produced in the craftsmanship part when the parameters are correctly inputted for the robotic arm to be produced.

In this study, a design for a lightweight, portable MIG welding robotic arm that can be easily mounted in different positions and perform welding tasks, particularly for use in various applications including the automotive and defense industries, has been prepared using the SOLIDWORKS® program (Karaca et al., 2017). Towards this goal, initially, the system's mechanism, necessary power calculations, usage of the method, and motion scheme were established. The determined requirements were researched and their analyses were conducted using ANSYS® software (Tınkır and Sezgen, 2017). A geometric and kinematic model suitable for the industrial and factory environment in which the task will be carried out has been presented.

2. Materials and Methods

2.1. Material

In this study, different materials were selected for the torch and body parts of the designed MIG welding robotic arm, considering the cost factor. The selection of materials was crucial, because the power of

the motor to be used depends on the resulting weight. Therefore, the materials were chosen with minimum weight and maximum efficiency in mind. Careful selection of the material for production is necessary. In material selection, aside from high performance, flexibility, machinability, and strength characteristics have been important guides for the engineers selecting the material. In the designed robotic arm, as shown in Figure 1, polylactic acid (PLA) materials obtained by the additive manufacturing method were used in the body and limbs.

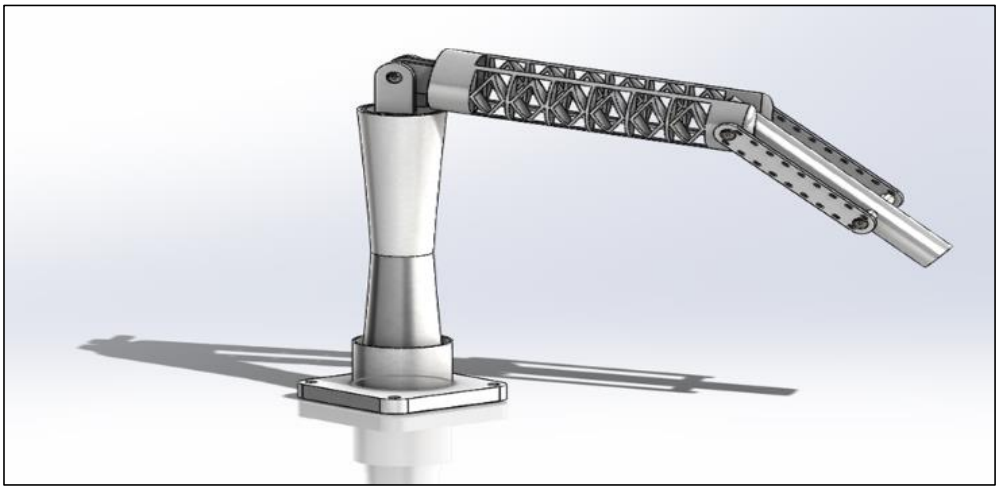

Figure 1. Robotic arm limb and body structure

Table 1. Mechanical and physical properties of PLA material (Farah et al., 2016)

Property	Value
Density	1.25 g/cm³
Melting temperature	150-160°C
Tensile strength	50-70 MPa
Elastic modulus (e-modulus)	3-4 GPa
Notched impact strength	2-16 kJ/m² (low impact resistance)
Maximum stress strength	50 MPa
Elongation (at break)	2-10%
Flexural strength	65-110 MPa
Water absorption (24 hours)	0.5 - 1.0%
Glass transition temperature	60-65°C
Thermal expansion coefficient	68 µm/m°C
Shore hardness	80-85D
Processability	Easy

The use of 3D printers has become easier in many sectors by combining materials with different properties using filaments produced through additive manufacturing methods. It is used primarily in the textile industry for the production of wearable gloves (Akgümüş Gök and Güdar, 2023), composite

material production (Pamuk et al., 2016), and more recently in the production of robotic arms (Çelebi et al., 2019). The choice of material for the robotic arm may vary depending on the task it will perform. Within the scope of this study, PLA materials that can be used in 3D printers were selected for the manufacturing of this robotic arm. In the design of the MIG welding robotic arm, the most important point in material selection is the choice of the torch material. The selection of torch material results in high-quality welding. When selecting the torch, a torch design was prepared, taking into account factors, such as the maximum power of the current generator, the diameter of the wire electrode to be used, the thickness of the material to be welded, the working time, ergonomics, and is represented in Figure 2 (Suarez et al., 2017). Apart from the general material of the torch being insulating, the mouthpiece where welding contact occurs is expected to be resistant to high temperatures and absorb the generated heat to prevent overheating and deformation of other parts of the arm. To achieve this, airflow gaps were left at various points on the torch to ensure continuous airflow.

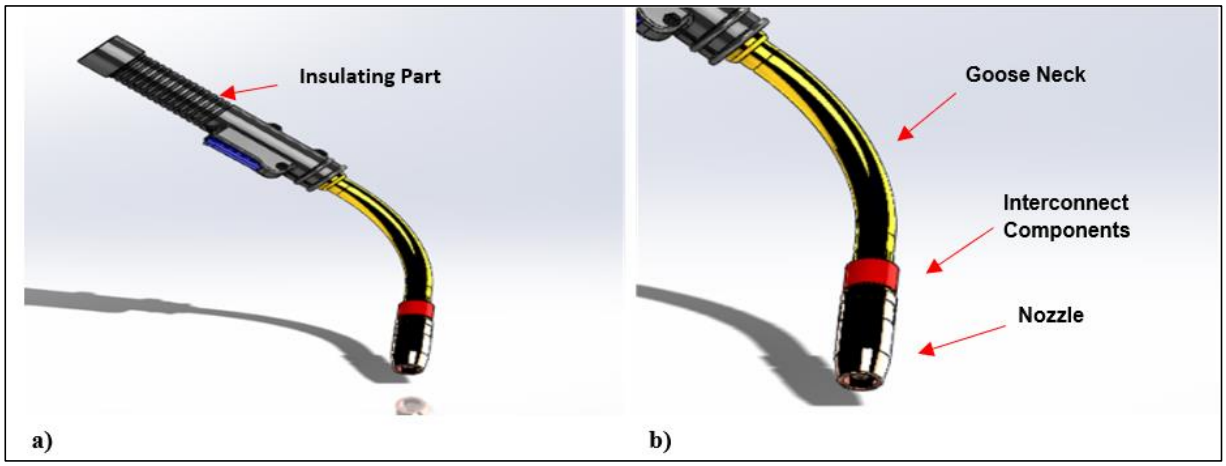

Figure 2. a) Insulating part of the torch, **b)** Conductive part of the torch

The upper part of the torch, which needs to have insulating properties, was selected to be made of acrylonitrile butadiene styrene (ABS) plastic due to its cost-effectiveness. The yellow part referred to as the (Goose Neck) was determined to be made of brass, following traditional torch manufacturing methods. The most important factor in this selection is that since welding is done with electricity, conductivity needs to be good at a certain point. This part serves the purpose of absorbing the energy of the heated electrode. In the tip of the torch, the intermediate connecting part was made of brass, and the nozzle itself was made of copper material.

2.2. Design

Today, the designs of machines or machine components are done in digital environments using computer aided design (CAD) programs to facilitate manufacturing. SOLIDWORKS® is an internationally used program that allows design in various applications such as sheet metal, molds, profiles, and electronics. The design of the MIG welding robotic arm was done in the SOLIDWORKS® program. In the design,

geometric voids were created, as shown in Figure 3, to achieve the desired weights without compromising strength. These geometric voids were created in a way that would not affect the strength and material fatigue (Ertürkmen and Noori, 2023).

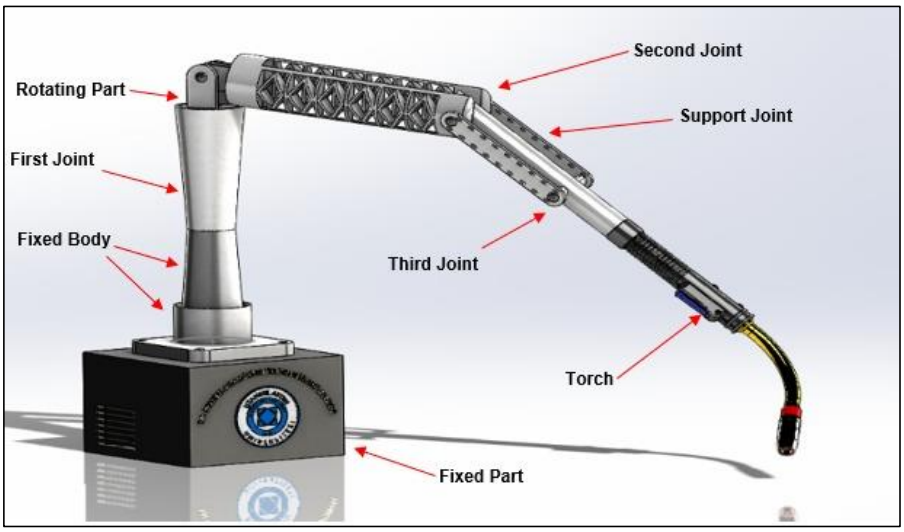

Figure 3. Configuration created with the design program for the robotic arm

Due to the limited electronic and mechanical power of the system, this was taken into account during the design and the design was carried out accordingly. When considering its maximum load capacity, the length of the welding torch head was designed to be 22.11 cm. The maximum welding length that can be achieved is 45 cm. As a result of the dynamic analyses conducted, the number and type of motors to be used have been determined.

Serial robot types are also classified alphabetically based on the type of joint (limb) they have. Generally, there are two types of joints: rotary and prismatic joints. Rotary joints are symbolized by the letter "R" (Revolute), while prismatic joints are symbolized by the letter "P" (Prismatic). The MIG welding robotic arm was designed as an RRRR robot (Can and Stachel, 2014). In the design of the robotic arm, 3 joints, 2 rotation support parts, and 2 motion transmission support members were used. The design of these parts took into consideration the load, mobility, and durability that the robotic arm would be subjected to. The length of the first main joint is 30 cm, and it consists of a straight cylinder part that is symmetrically conical, as shown in Figure 4. The reason for this is to distribute the load less on the side with a larger surface area.

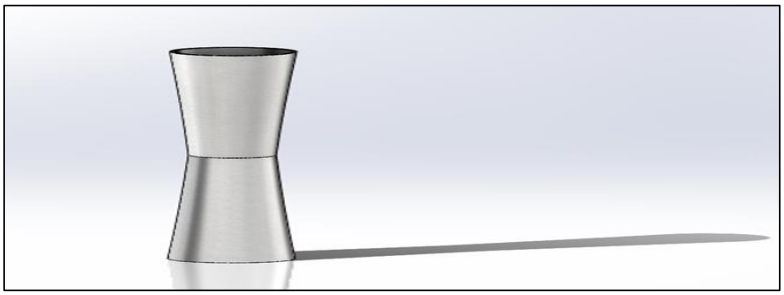

Figure 4. First joint

The length of the second joint in the design is 35 cm. As seen in Figure 5, rectangular voids of equal dimensions were left to improve maneuverability, speed, and weight.

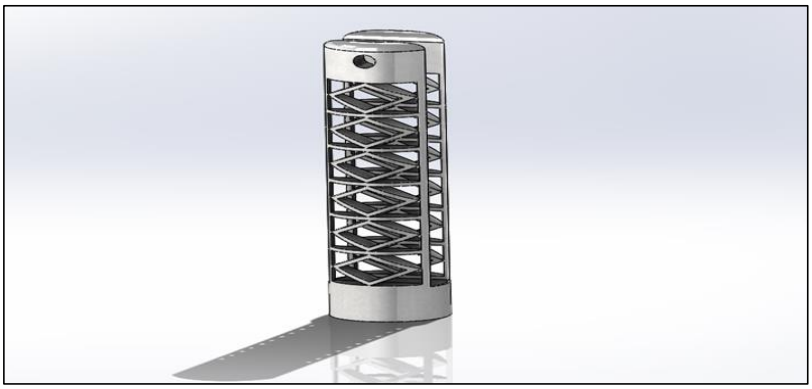

Figure 5. Second joint

The third and final joint, as seen in Figure 6, is a straight cylindrical part designed entirely according to the task's purpose. This part, which is 20 cm in length, is primarily responsible for ensuring that the welding wire coming from the spool reaches the nozzle smoothly.

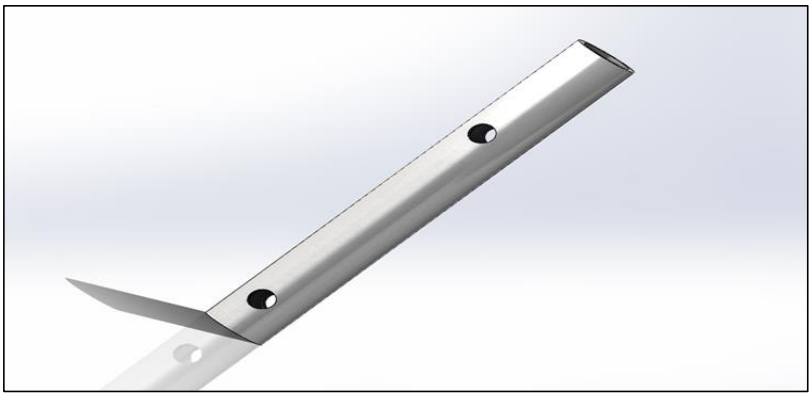

Figure 6. Third joint

The length of the motion transmission support members is 10 cm, and their roles in the design are to support the correct transmission of motion, ensure more balanced movement of the load, and increase speed. As shown in Figure 7, the design includes slot voids at the top and bottom to enhance strength.

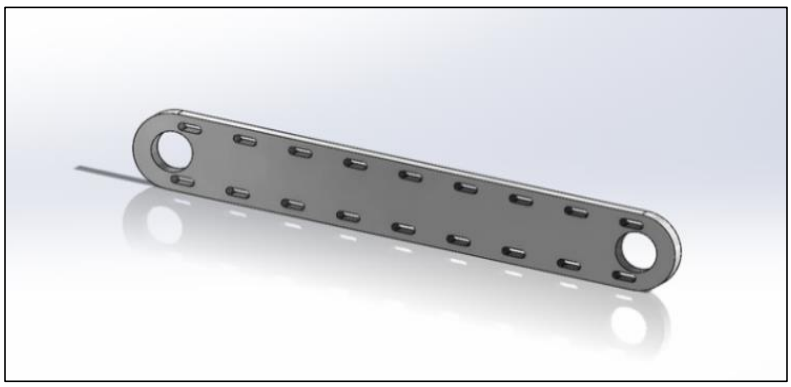

Figure 7. Motion transmission support member

2.3. Analysis

In this study, a comprehensive structural analysis was carried out to examine the performance and deformation behavior of the joints used in the design of the MIG welding robot arm. Analyzes were performed using both SOLIDWORKS® and ANSYS® programs to evaluate how the design responds under operating conditions. The mesh structure used in the analysis was optimized to accurately model the complex geometry of the robot arm. Three-dimensional solid elements were used in the analyses. Tetrahedral elements are preferred because these elements give better results in complex geometries. Different resolutions were used in different regions with element sizes ranging from 0.5 mm to 3 mm. Sensitivity has been increased by using smaller elements in critical load-bearing areas. More than 100.000 elements were used in total. The mesh used in this study was optimized in terms of quality and provided sufficient resolution for more accurate calculation of deformations and stresses. The number of meshes was created as 7000 in the first joint and 2500 in the second joint. Figure 8 shows the mesh structure of the second joint.

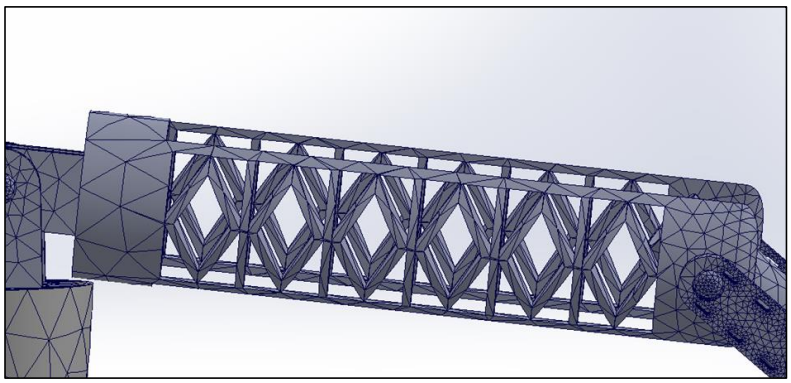

Figure 8. Mesh structure of second joint

The material model used in the analysis was chosen to accurately represent the materials used in prototype production. The robot arm and joints are produced using PLA material. For this reason, the mechanical properties of PLA material were used in the analysis (Table 1). In the analysis of the robot arm, loads and boundary conditions are carefully defined. Forces of different magnitudes were applied to evaluate the effect of loads on the joint. Each loading case is designed to simulate real operating conditions of the robot arm. Loads weighing 200 g, 300 g and 400 g were applied to the free end of the arm. These loads were chosen to simulate the maximum loads that the robot arm can carry. The points where the arm is fixed are defined as boundary conditions and it is assumed that these points do not move. The gravitational force is taken into account for realistic modeling of the robot arm. Static and dynamic analyzes were used in structural analysis. Loads were applied in a fixed condition and deformation, stress and deflections were calculated. This analysis was used to evaluate the maximum tensile strength and load carrying capacity of the arm. Using the ANSYS® Rigid Dynamics module, dynamic forces and deformations occurring during the movement of the arm were examined. This analysis tested the performance of the moving parts of the arm at different angles. As a result of the analyses, the deformation and tension behaviors of the robot arm were determined. The results obtained

in each loading scenario played an important role in evaluating how the robot arm performed under different operating conditions. Deformations and stresses observed especially in critical joints revealed the weak points of the design and data for future optimization studies are presented in the "Results" section.

3. Advanced Kinematic Modeling and Power Calculations

The Denavit-Hartenberg (DH) method was used for modeling all forward kinematics and mechanical connections of the designed system (Noguchi and Roshanianfard, 2017). Power-moment calculations were performed for the created MIG welding robotic arm. In the designed robotic arm, there are no translational mechanical movements in any joint, and all mechanical joints are rotational. In this case, the position vector in joint space, **q**, is directly equivalent to a velocity vector, **v**, meaning **q** = [q1 ... qn] = [v1 ... vn] = **v**. Mathematically, this relationship can be expressed briefly as **q**˘ = **Hq**, where **q**˘ is the motor position, **H** is the matrix that transforms joint space to motor space. For the designed robotic arm, the **H** matrix is a 6 × 5 matrix, and the determinant of this matrix is greater than zero. Furthermore, to create a comprehensive expression, after the robotic arm is manufactured, tests need to be conducted based on the system's dynamics. System identification tests can be used to draw the entire kinematic and dynamic model of the robotic arm system. The direct kinematic expression of the robotic arm is given by the transformation matrix **T** (Korkut and Yaşar, 2016).

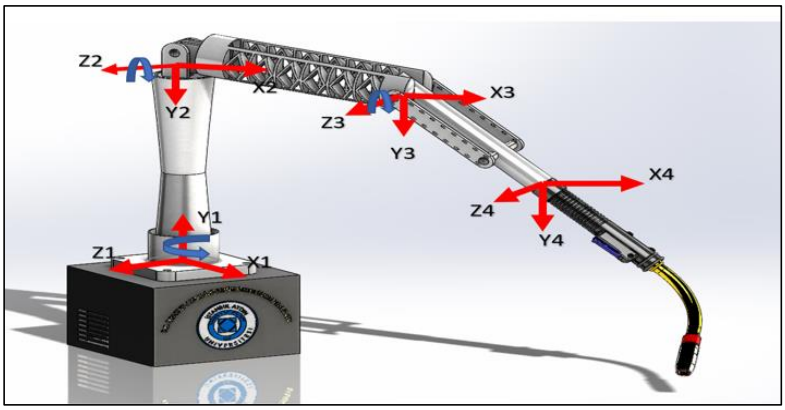

Figure 9. Kinematic vectors of the robot arm

In order to perform forward and inverse kinematic analysis of a robotic arm, the axes must first be determined. In the design done in SOLIDWORKS® program, the axes and rotation directions of the robotic arm are shown as in Figure 9.

Table 2. Denavit-Hartenberg (DH) table

Frame	$\alpha_{(i-1)}$	$a_{(i-1)}$	$d_{(i-1)}$	$\theta_{(i-1)}$
0-1	0	0	0	$\theta_{(1)}$
1-2	0	L_1	0	$\theta_{(2)}$
2-3	0	L_2	0	$\theta_{(3)}$
3-4	0	L_3	0	$\theta_{(4)}$

After the axes were established, rotation and translation distances, angles, and lengths were determined using the Denavit-Hartenberg (DH) method. The transformation matrices **T** were created by referencing the Table 2 generated with the Denavit-Hartenberg (DH) method.

In this study, a mesh was created using Solidworks Motion Study and ANSYS Rigid Dynamic module for analysis, and data about the designs was obtained by entering the necessary parameters. These data obtained largely show the prototype production and deformations that may occur in the system. As a result of these analyses, many data such as deviations, bending and maximum movement area in robot arm designs were obtained. In future studies, it is recommended to present the mathematical expressions of the kinematic model, dynamic matrices and transformation matrices in more detail. In addition, using the MATLAB program, forward kinematic and inverse kinematic analysis can be used to mathematically calculate the relative movements, positions, orientations, speeds and resulting inertia of the robot arm. Figure 10 shows the advanced kinematic analysis created using the MATLAB program of the study.

```
clear; clc; close;

link=1:1:7;
h_base= [0,1,0;
        0,1,0;
        1,0,0;
        0,0,1;
        1,0,0;
        1,0,0;
        1,0,0];
syms d1_d th2_d th3_d th4_d th5_d th6_d mx my mz xx yy zz
syms a1 k2 k3 k4 a5 a6 d1 d2 d3 d4 d5 d6 teta1 teta2 teta3 teta4 teta5 teta6 l1
syms d1_dd th2_dd th3_dd th4_dd th5_dd th6_dd

I=eye(3);

z=zeros(3,1);
w0=zeros(3,1);
v0=zeros(3,1);
wd0=zeros(3,1);
vd0=zeros(3,1);
f0=zeros(3,1);
sqew=@(x) [0 -x(3) x(2); x(3) -x(1) 0; x(2) -x(1) 0];
m=[mx,0,0;0,my,0;0,0,mz];
I_m=[xx,0,0;0,yy,0;0,0,zz];
```

```
h1=[0;1;0];
h11=[h1;z];
h2=[0;1;0];
h22=[h2;z];
h3=[1;0;0];
h33=[h3;z];
h4=[0;0;1];
h44=[z;h4];
h5=[1;0;0];
h55=[h5;z];
h6=[1;0;0];
h66=[z;h6];
h7=[1;0;0];
h77=[h7;z];

l1_v=h1*link(1);
l2_v=h2*link(2);
l3_v=h3*link(3);
l4_v=h4*link(4);
l5_v=h5*link(5);
l6_v=h6*link(6);
l7_v=h7*link(7);

phi1=[I,zeros(3);-sqew(l1_v),I];
phi2=[I,zeros(3);-sqew(l2_v),I];
phi3=[I,zeros(3);-sqew(l3_v),I];
phi4=[I,zeros(3);-sqew(l4_v),I];
phi5=[I,zeros(3);-sqew(l5_v),I];
phi6=[I,zeros(3);-sqew(l6_v),I];

V_vv1=phi1*zeros(6,1)+h11*d1_d;
V_vv2=phi2*zeros(6,1)+h22*th2_d;
V_vv3=phi3*zeros(6,1)+h33*th3_d;
V_vv4=phi4*zeros(6,1)+h44*th4_d;
V_vv5=phi5*zeros(6,1)+h55*th5_d;
V_vv6=phi6*zeros(6,1)+h66*th6_d;

w1=V_vv1(1:3,1);
w2=V_vv2(1:3,1);
w3=V_vv3(1:3,1);
w4=V_vv4(1:3,1);
w5=V_vv5(1:3,1);
w6=V_vv6(1:3,1);

v1=V_vv1(4:6,1);
v2=V_vv2(4:6,1);
v3=V_vv3(4:6,1);
v4=V_vv4(4:6,1);
v5=V_vv5(4:6,1);
v6=V_vv6(4:6,1);

A_vv1=phi1*zeros(6,1)+h11*d1_dd+[cross(w0,w1);cross(w0,cross(w0,l1_v))];
A_vv2=phi2*A_vv1+h22*th2_dd+[cross(w1,w2);cross(w1,cross(w1,l2_v))];
A_vv3=phi3*A_vv2+h33*th3_dd+[cross(w2,w3);cross(w2,cross(w2,l3_v))];
A_vv4=phi4*A_vv3+h44*th4_dd+[cross(w3,w4);cross(w3,cross(w3,l4_v))];
A_vv5=phi5*A_vv4+h55*th5_dd+[cross(w4,w5);cross(w4,cross(w4,l5_v))];
A_vv6=phi6*A_vv5+h66*th6_dd+[cross(w5,w6);cross(w5,cross(w5,l6_v))];

V_=[V_vv1;V_vv2;V_vv3;V_vv4;V_vv5;V_vv6];
```

```
A_=[A_vv1;A_vv2;A_vv3;A_vv4;A_vv5;A_vv6];

PHI=eye(18,18);

PHI(7:12,1:6)=phi2;
PHI(7:12,7:12)=phi2;
PHI(13:18,1:6)=phi2*phi3;

M1=[I_m,m*sqew(l1_v/2);-m*sqew(l1_v/2);I*m];
M2=[I_m,m*sqew(l2_v/2);-m*sqew(l2_v/2);I*m];
M3=[I_m,m*sqew(l3_v/2);-m*sqew(l3_v/2);I*m];
M4=[I_m,m*sqew(l4_v/2);-m*sqew(l4_v/2);I*m];
M5=[I_m,m*sqew(l5_v/2);-m*sqew(l5_v/2);I*m];
M6=[I_m,m*sqew(l6_v/2);-m*sqew(l6_v/2);I*m];

x1= [0 90 -90 0 -90 90];
a=  [0 0 0 k3 k4 0 ];
d=  [l1 (k2+d2) 0 0 0 d6];
t=  [teta1 teta2 teta3 teta4 teta5 teta6];

for i=1:6
   if i== 1
      T1= [cosd(t(i)) -sind(t(i)) 0 a(i) ;
          cosd(x1(i))*sind(t(i)) cosd(x1(i))*cosd(t(i)) -sind(x1(i)) -sind(x1(i))*d(i) ;
          sind(t(i))*sind(x1(i)) cosd(t(i))*sind(x1(i)) cosd(x1(i)) cosd(x1(i))*d(i) ;
          0 0 0 1];
   elseif i== 2
      T2= [cosd(t(i)) -sind(t(i)) 0 a(i) ;
          cosd(x1(i))*sind(t(i)) cosd(x1(i))*cosd(t(i)) -sind(x1(i)) -sind(x1(i))*d(i) ;
          sind(t(i))*sind(x1(i)) cosd(t(i))*sind(x1(i)) cosd(x1(i)) cosd(x1(i))*d(i) ;
          0 0 0 1];
   elseif i==3
      T3= [cosd(t(i)) -sind(t(i)) 0 a(i) ;
          cosd(x1(i))*sind(t(i)) cosd(x1(i))*cosd(t(i)) -sind(x1(i)) -sind(x1(i))*d(i) ;
          sind(t(i))*sind(x1(i)) cosd(t(i))*sind(x1(i)) cosd(x1(i)) cosd(x1(i))*d(i) ;
          0 0 0 1];
   elseif i==4
      T4= [cosd(t(i)) -sind(t(i)) 0 a(i) ;
          cosd(x1(i))*sind(t(i)) cosd(x1(i))*cosd(t(i)) -sind(x1(i)) -sind(x1(i))*d(i) ;
          sind(t(i))*sind(x1(i)) cosd(t(i))*sind(x1(i)) cosd(x1(i)) cosd(x1(i))*d(i) ;
          0 0 0 1];
   elseif i==5
      T5= [cosd(t(i)) -sind(t(i)) 0 a(i) ;
          cosd(x1(i))*sind(t(i)) cosd(x1(i))*cosd(t(i)) -sind(x1(i)) -sind(x1(i))*d(i) ;
          sind(t(i))*sind(x1(i)) cosd(t(i))*sind(x1(i)) cosd(x1(i)) cosd(x1(i))*d(i) ;
          0 0 0 1];
   elseif i==6
      T6= [cosd(t(i)) -sind(t(i)) 0 a(i) ;
          cosd(x1(i))*sind(t(i)) cosd(x1(i))*cosd(t(i)) -sind(x1(i)) -sind(x1(i))*d(i) ;
          sind(t(i))*sind(x1(i)) cosd(t(i))*sind(x1(i)) cosd(x1(i)) cosd(x1(i))*d(i) ;
          0 0 0 1];
   end
end
```

Figure 10. Advanced kinematic analysis for robot arm designs

4. Prototype Model

Before manufacturing a robotic arm, design analysis and calculations must be made. If no problems are observed after calculations, design and analysis, the manufacturing phase can be started and prototype

testing can be done. The parts of the designed MIG welding robotic arm produced by a 3D printer are shown in Figure 11.

Figure 11. Parts produced by a 3D printer

In the SOLIDWORKS® environment, it is planned to safely carry out the required load-carrying process by attaching MG996r high-torque servo motors (Figure 12) to the movable joints of the parts made.

Figure 12. MG996r servo motor

For the electronic software, an Arduino Mega board has been used. The software was written in the Arduino IDE environment by invoking Bluetooth and servo libraries, as shown in Figure 13.

```
#include <SoftwareSerial.h>
#include <Servo.h>

Servo servo01;
Servo servo02;
Servo servo03;
Servo servo04;
Servo servo05;
Servo servo06;

SoftwareSerial Bluetooth(0, 1); // Arduino(RX, TX) - HC-05 Bluetooth (TX, RX)
```

```
int  servo1Pos, servo2Pos, servo3Pos, servo4Pos, servo5Pos, servo6Pos;
int  servo1PPos, servo2PPos, servo3PPos, servo4PPos, servo5PPos, servo6PPos;
int  servo01SP[50], servo02SP[50], servo03SP[50], */servo04SP[50], servo05SP[50], servo06SP[50];
int speedDelay = 20;
int index = 0;
String dataIn = "";

void setup() {
  servo01.attach(8);
  servo02.attach(9);
  servo03.attach(10);
  servo04.attach(11);
  servo05.attach(12);
  servo06.attach(13);
  Bluetooth.begin(9600); // Baud Rate
  Bluetooth.setTimeout(1);
  delay(20);
  // Robot kol ilk pozisyon
  servo1PPos = 90;
  servo01.write(servo1PPos);
  servo2PPos = 150;
  servo02.write(servo2PPos);
  servo3PPos = 35;
  servo03.write(servo3PPos);
  servo4PPos = 140;
  servo04.write(servo4PPos);
  servo5PPos = 85;
  servo05.write(servo5PPos);
  servo6PPos = 80;
  servo06.write(servo6PPos);
}
```

Figure 13. Software program used for the prototype

An android package kit (APK) application has been prepared for the system to be actively used. Since the Arduino reduces the incoming voltage to 2.5 volts, the "+" and "-" voltages in the motors have been integrated into a separate system. A motor driver was used to prevent frequency fluctuations in the motors and to stabilize the voltage supplied to the motors. The Arduino Mega and the motors are directly powered by 5V. All electronic and mechanical materials used for the prototype test are shown in Figure 14.

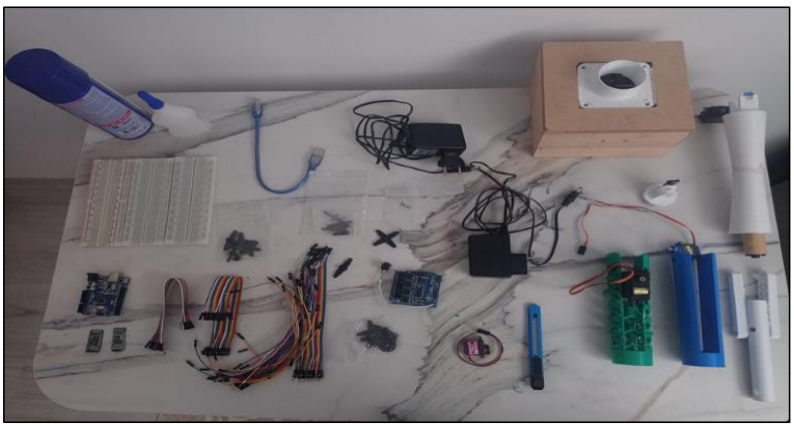

Figure 14. All materials used for the prototype test

The prototype prepared as a result of combining the electronic and mechanical connections of the product, which emerged with the necessary software and applications for the operation of the designed robotic arm, has been made suitable for trial runs as seen in Figure 15.

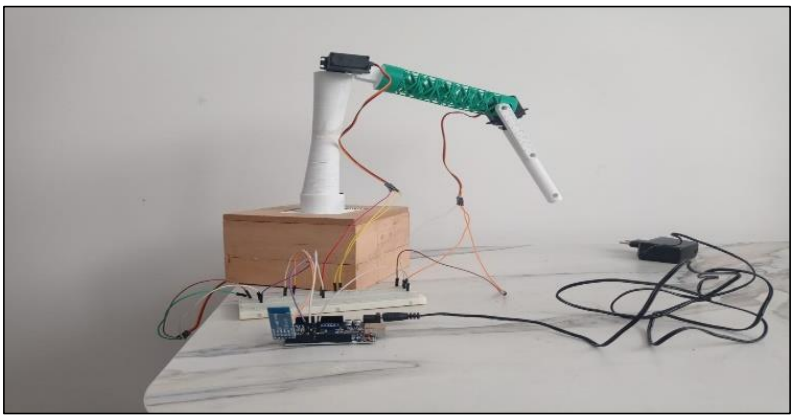

Figure 15. Created prototype model

MIG welding system is a heavy and complex system. In the system, the torch, connection cable, welding control box and the conductive metal attached to the torch constitute the main parts of the system. There is an on-off button on the welding torches for safety. The whole system is shown in Figure 16.

Figure 16. Main elements of the welding torch system

For active operation of the system, all activations of the electronic components were transferred to the electronic card circuit. The first code written for security purposes was written to direct the robot to a standard specific location. This starting position is shown in Figure 17.

Figure 17. Starting position of welding torch

By calculating the movement and maneuver area of the robot arm, a floor on which it could perform the operation was determined. The working principle is to follow the welding path on this ground and complete the welding task. For this purpose, the process steps were started from the starting position and followed the welding path in each welding region, and each step was recorded with the SAVE command. After all movements are recorded, the robot arm follows the previously recorded path over and over again with the RUN command in Figure 18.

Figure 18. Robot arm while doing MIG welding

The welded parts made by the prototype model MIG welding robot during the trial runs are shown in Figure 19 before welding and Figure 20 after welding. For welding, the surface of the material must first be cleaned. And before the material is welded, it must be attached to the place to be welded with a spot and the surface flatness must be checked.

Figure 19. The part to be welded

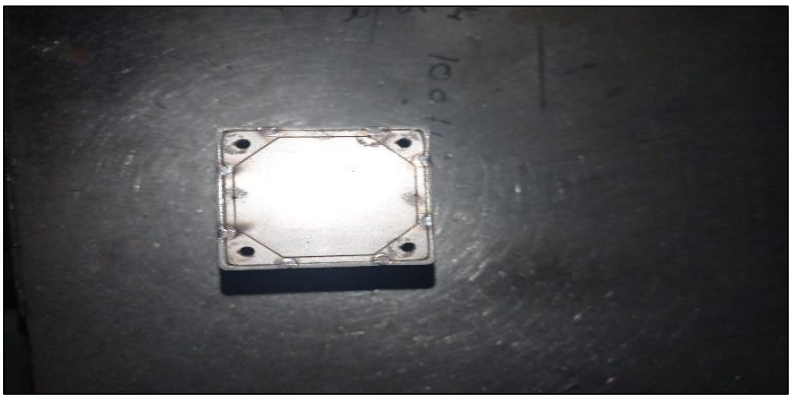

Figure 20. Workpiece after welding

5. Analysis and Results

For the analysis of the designed robotic arm, the second joint was selected. The reason for selecting this joint is that it forms the connection point between the first and third joints in the design and is the limb with the most important function in this respect. Since this joint plays a critical role in the movement and load-carrying capacity of the robot arm, it directly affects the overall performance and precision during welding operations. Therefore, the stiffness of this joint significantly affects the efficiency and precision of the robot arm. SOLIDWORKS® program were used to analyze the deformation images and deviation graphs resulting from the application of loads of different magnitudes on the meshed joint. In SOLIDWORKS®, the direction of gravity was determined, and a fixed fixture was set. The material was chosen as PLA. Deformation images and bends were observed by applying a force equal to the weight of the torque at the free end and two loads greater than its own value proportionally. Initially, the deformations and deviations caused by three different loads of 200 g, 300 g, and 400 g, in addition to the standard torque (based on dimensions and materials) and the weight of the arm, were examined.

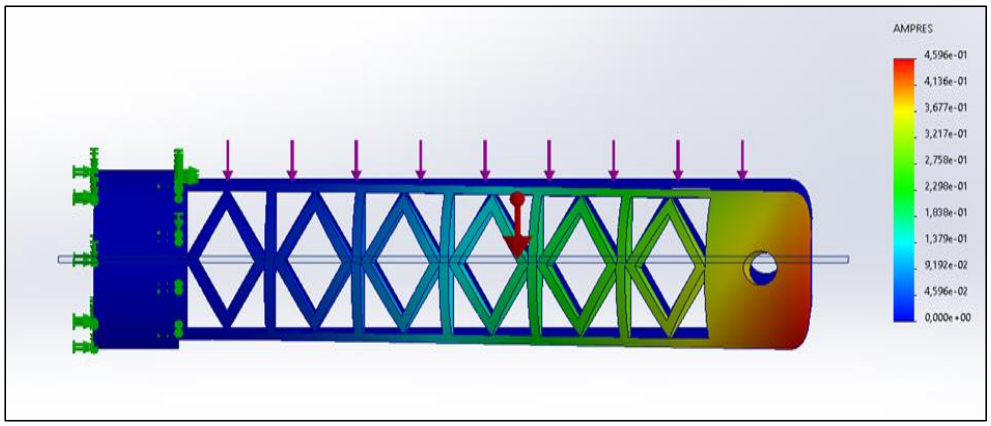

Figure 21. Deformation graph and bending results from the first load

As shown in Figure 21, in the first load (200 g) analysis, it was observed that the deviation (deformation) at the minimum applied load was a maximum of 4.596 mm. The deformation in the material occurred outward and downward from the center of the joint. This low level of deformation indicates that the robotic arm can operate under small loads without significant degradation. However, even this level of loads can cause material fatigue over long periods of use, which can affect the durability of the arm in the long term.

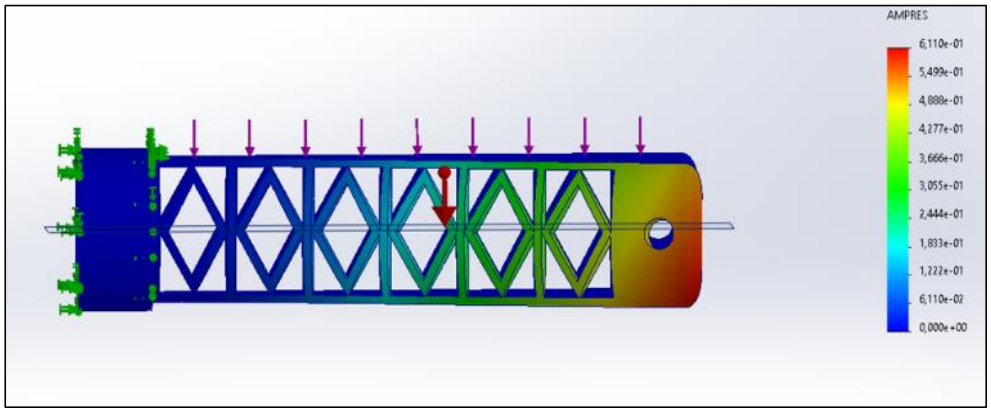

Figure 22. Deformation graph and bending results from the second load

As shown in Figure 22, in the analysis of the second load (300 g), it was observed that the deviation (deformation) at the minimum applied load was a maximum of 6.110 mm. The deformation in the material occurred outward and downward from the center of the joint. This increased deflection indicates that the joint exhibits flexibility at higher loads and may negatively affect the accuracy of welding operations. Although this level of deformation is still within acceptable limits, optimizing joint strength will be important to minimize loss of sensitivity. This result suggests that although PLA material is suitable for 3D printing, it may show limitations when approaching the load limits under the operating conditions of the robot arm. For situations where higher load capacities are required, strengthening the material or using alternative materials may be considered in future designs.

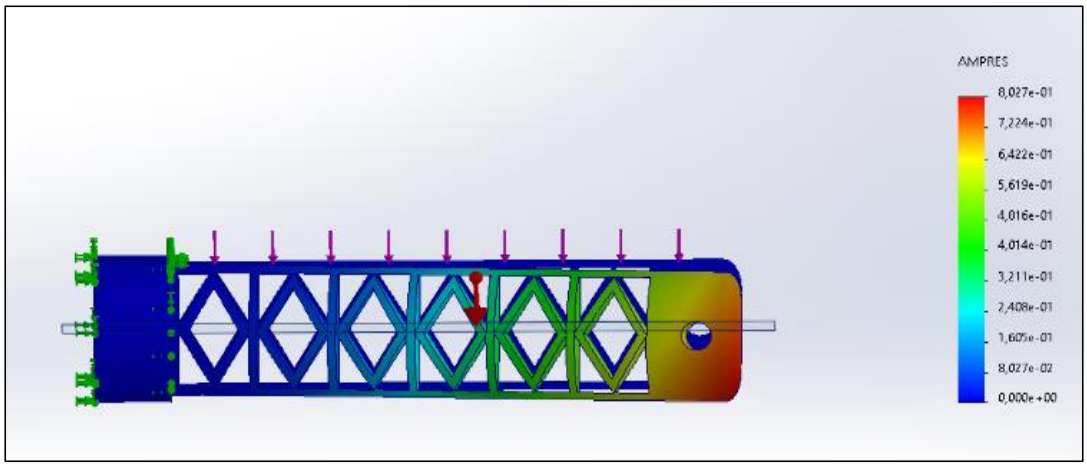

Figure 23. Deformation graph and bending results from the third load

As shown in Figure 23, in the analysis of the third load (400 g), it was observed that the deviation (deformation) at the minimum applied load was a maximum of 8.027 mm. The deformation in the material occurred outward and downward from the center of the joint. This degree of deformation indicates that the arm may have difficulty maintaining its sensitivity in welding operations at this load level. The increased deformation also indicates that the PLA material is approaching its limits for this design.

These analyzes show that the robot arm can function under heavier loads, but the precision of welding operations may be compromised. Optimizing the load-carrying capacity and reinforcing it in future designs is recommended to ensure both precision and reliability under maximum operating conditions. Materials with higher strength-to-weight ratio, such as carbon fiber composites, or the use of metal-based 3D printing may contribute to solving the problems observed in these tests.

For the comparison and evaluation of the results, as seen in Figure 24, a mesh was applied to first joint in the ANSYS® program, and the system's maximum bending and deformation graphs were generated.

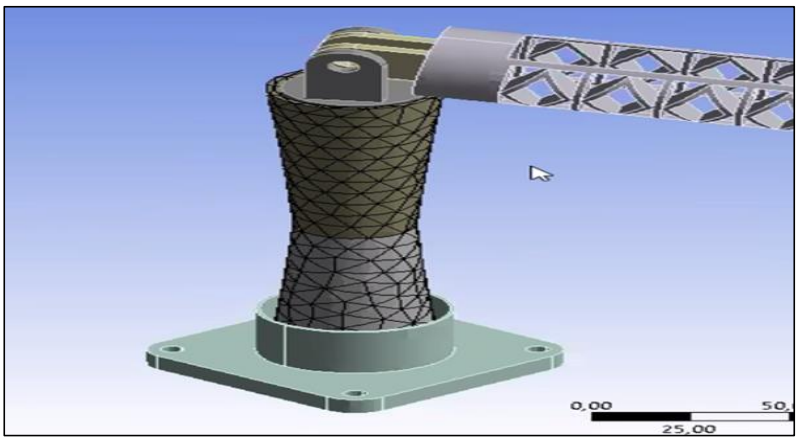

Figure 24. Creating ANSYS® mesh

After the meshing process, the deformation (deviation) and load analysis results on first joint of the MIG welding robotic arm, which underwent motion simulation at specified angles, are shown in Figures 25 and 26.

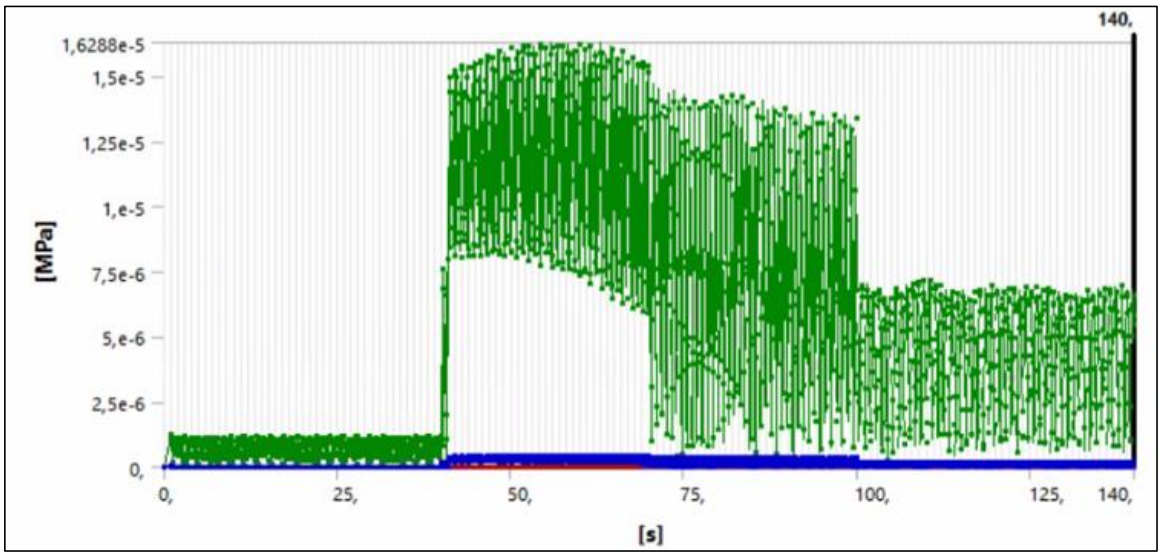

Figure 25. Maximum stress graph

As seen in Figure 25, the maximum stress experienced by the second and third joints between 0° and 90° is shown in the graph. These stress concentrations highlight critical points where material fatigue or failure may occur during long-term use.

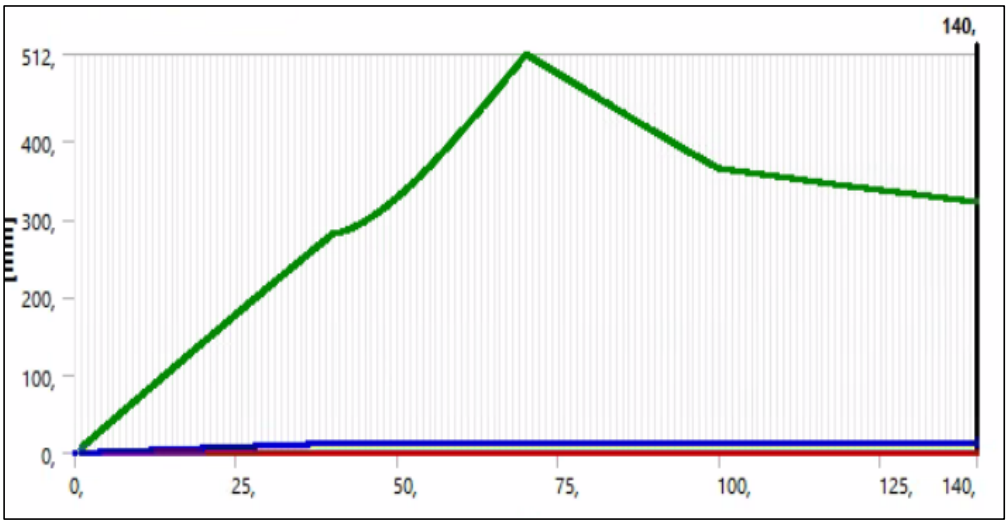

Figure 26. Maximum deviation graph

As seen in Figure 26, the total deviation that occurred in first limb was calculated as 344 mm. This deviation and the calculated total movement time of 140 seconds demonstrate the dynamic behavior of the arm during operation. Deflection indicates the accumulation of stress in the joint throughout the movement cycle and highlights the need for design strengthening or advanced material selection to reduce these effects.

6. Conclusions

In this study, a lightweight and portable robot arm capable of MIG welding was designed and analyzed for use in the automotive and defense sectors. The design of the robot arm was carried out using the SOLIDWORKS® program and the material selection was made taking into account weight, strength and cost efficiency. While PLA material was preferred for the body and joints of the arm due to its mechanical properties suitable for the 3D printing process, ABS and brass were used in the components of the welding torch to ensure heat resistance and conductivity.

Kinematic modeling of the robot arm was carried out with the Denavit-Hartenberg (DH) method and kinematic and dynamic analyzes were performed to optimize its functionality. SOLIDWORKS® and ANSYS® softwares were used together to simulate the mechanical behavior of the arm under different load conditions. After designing in the SOLIDWORKS® program, the analyses conducted on the second limb showed a deviation of 4.596 mm for a 200 g material under a 2 N load, 6.110 mm deviation for a 300 g material under a 3 N load, and 8.027 mm deviation for a 400 g material under a 4 N load. Analysis results showed that the arm performed well at moderate loads, but significant deformation and stresses occurred in critical joints at higher loads. These findings reveal that the current design is suitable for light duty, but optimization in material selection and joint reinforcement is required for applications requiring heavy loads. In the analyses conducted in the ANSYS® program for the first limb of the designed MIG welding robotic arm, the maximum deviation experienced by the first limb during a motion simulation at different angles for 140 seconds was calculated to be 344 mm. This situation can be considered as an issue that can be rectified by having the robotic arm first indicate the welding coordinates and then perform the welding. In the same analysis, the maximum stress occurring was calculated as 1.6288e-5 MPa, which is a very small value, indicating that the system can operate healthily for a long period.

As a result, the designed MIG welding robot arm offers a promising solution for tasks requiring mobility and flexibility, especially in environments where human intervention is risky. However, future studies should focus on alternative materials such as carbon fiber composites or metal-based 3D printing to increase the load-bearing capacity and deformation resistance of the arm. Additionally, it would be beneficial to develop kinematic and dynamic models with more detailed mathematical expressions to increase the sensitivity of the robot arm and its adaptability to industrial-scale applications.

References

Akgümüş Gök D., Güdar B. Computational analysis wearable glove produced with FDM technology. Proceedings of the International Conference on Science, Engineering Management and Information Technology (SEMIT) 2023; 134, Ankara.

Bakırcı M., Demiray A. Pre-production design of a robotic arm mounted on an unmanned aerial vehicle (UAV). Computational Intelligence, Data Analytics and Applications 2023; 1-8.

Barnett J., Duke M., Au CK., Lim SH. Work distribution of multiple Cartesian robot arms for kiwifruit harvesting. Computers and Electronics in Agriculture 2020; 169(105202): 1-9.

Can E., Stachel H. A planar parallel 3-RRR robot with synchronously driven cranks. Mechanism and Machine Theory 2014; 79: 25-42.

Çelebi A., Korkmaz A., Yılmaz T., Tosun H. Design and production of 6 axis robot arm by 3D printer. International Journal of 3D Printing Technologies and Digital Industry 2019; 3(3): 269-278.

Doruk E., Pakdil M., Çam G., Durgun İ., Kumru UC. Otomotiv sektöründe direnç nokta kaynağı uygulamaları. Mühendis ve Makina 2016; 57(673): 2-6.

Efe E., Özcan M., Haklı H. Building and cost analysis of an industrial automation system using industrial robots and PLC integration. European Journal of Science and Technology 2021; 28: 1-10.

Ertürkmen E., Noori AR. Free vibration analysis of curved castellated beams with different geometric web openings by the finite element method. Gümüşhane University Journal of Science and Technology 2023; 13(4): 1019-1032.

Farah S., Anderson DG., Langer R. Physical and mechanical properties of PLA, and their functions in widespread applications - A comprehensive review. Advanced Drug Delivery Reviews 2016; 107: 367-392.

Karaca F., Akmeşe F., Ünal E. Kinetic and kinematic analysis of the lower extremity stand to sit. International Journal of Innovative Engineering Applications 2021; 5(1): 32-35.

Karacan AN., Şahin Hİ., Özmen M. Multi-objective assembly line balancing with human-robot collaboration. Adıyaman University Journal of Engineering Sciences 2022; 16: 10-36.

Korkut I., Yaşar SA. Design and kinematic analysis of a RRPR robot arm. International Journal of Innovative Research in Engineering & Management (IJIREM) 2016; 3(6): 491-492.

Köse C., Tatlı Z. The effect of welding speed on the mechanical and microstructure properties of robotic GMAW welded 5754 aluminium alloy. NWSA-Technological Applied Sciences 2015; 2-4.

Roshanianfard A., Noguchi N. Kinematics analysis and simulation of a 5DOF articulated robotic arm applied to heavy products harvesting. Journal of Agricultural Sciences 2017; 24(2018): 91-104.

Nurveren K., Gündüz BB. Investigation of microstructure and mechanical properties of 6082 aluminium alloy after MIG welding. Ömer Halisdemir University Journal of Engineering Sciences 2018; 7(2): 909-916.

Pamuk G., Kemiklioğlu U., Sayman O., Özdemir O. Low velocity impact response of biodegradable PLA composites reinforced by reclaimed cotton preforms. Textile and Apparel 2016; 26(3): 321-324.

Sarıyıldız SÖ., Demirhan A. Categorizing objects with image processing techniques and robot arm. Uludağ University Journal of The Faculty of Engineering 2021; 26(2): 547-554.

Suarez A., Soria PR., Heredia G., Arrue BC., Ollero A. Anthropomorphic, conformable and lightweight dual arm system for air manipulation. Proceedings of the IEEE/RSJ International Conference on Intelligent Robots and Systems 2017; 992-997. IEEE, Canada.

Tınkır M., Sezgen HÇ. Linear static analysis of hydraulic cylinder via finite element method. Ömer Halisdemir University Journal of Engineering Sciences 2017; 6(1): 3-5.

Türker M., Tosun M. Modern welding technologies used in the aerospace industry. Proceedings of the X. Welding Technology National Congress and Exhibition 2017; 123-130.